Asia-Pacific Journal of Science and Technology: Volume: 28. Issue: 01. Article ID.: APST-28-01-12. Research Article

APST

Asia-Pacific Journal of Science and Technology

https://www.tci-thaijo.org/index.php/APST/index

Published by the the Research and Graduate Studies,
Khon Kaen University, Thailand

Adsorption of Thioflavin T by nitrilotriacetic acid-modified activated carbon from water olive seeds

Chakkrit Umpuch[1,*], Supabhorn Jampa[1], Chonthicha Chaichan[1] and Channarong Puchongkawarin[1]

[1]Department of Chemical Engineering, Faculty of Engineering, Ubon Ratchathani University, Ubon Ratchatani, Thailand
[*]Corresponding author: chakkrit.u@ubu.ac.th

Received 22 July 2021
Revised 3 November 2021
Accepted 27 January 2022

Abstract

The adsorption of Thioflavin T (TT) dye from a solution was investigated using activated carbon (AC) made from water olive seeds and modified using nitrilotriacetic acid. The research was divided into three parts. Firstly, the specific surface area, average pore size, and total pore volume were calculated using the N_2 adsorption-desorption isotherm. The surface functional groups, surface morphology, and element content were characterized using a Fourier Transform Infrared Spectrophotometer and a Field Emission Scanning Electron Microscope. Secondly, influencing factors such as the initial pH solution, contact time, initial dye concentration, and temperature on the adsorption were investigated. The highest dye uptake of 43.09 mg/g was observed for the AC at the initial pH of 10.0, with a contact time of 240 min, an initial dye concentration of 50 mg/L and a temperature of 60°C. The dye uptake of the modified activated carbon (MAC) was 24.2 percent lower than that of the AC due to an increase in the surface charge density. Finally, the adsorption modeling was investigated. The experimental data followed the pseudo-second order kinetic model and Langmuir as well as Temkin isotherms. Although the modification of the AC using nitrilotriacetic acid reduces TT uptake, it increases the specific surface area of the MAC, which may increase sorption with regard to other pollutants.

Keywords: Thioflavin T dye, Activated carbon, Nitrilotriacetic acid, Water olive seed, Adsorption

1. Introduction

Synthetic dyes are used in many textile industries in the North-Eastern part of Thailand. Compared to natural dyes, synthetic dyes are preferred since they are cheap and available in the local market. In addition, bright and long-lasting clothing products can be produced with synthetic dyes [1]. Thioflavin T (TT) is one of the widely used synthetic dyes to color woven products such as silk, cotton, nylon, and acetate fiber [2]. Its structure is complex and contains hydrophilic functional groups such as amino groups. About half of the dyes used in the textile industry are discharged in the water after the dyeing process, becoming major sources of contamination. The high level of contamination can cause a negative impact on the environment, e.g., unpleasant smells and unsightliness [3]. Moreover, it can cause fatality or may produce serious damage to the health of the individual when exposed to the human body [4], therefore, it is necessary to treat the effluent prior to being discharged.

Adsorption is one of the most effective methods for the removal of synthetic dyes from liquid effluents. It is an effective approach because it is low-cost, fast, and easily applied. Activated carbon has been well-known as an adsorbent for decades and the cost of the commercial activated carbon is significantly lower than in the past according to analyses of activated carbon production costs [5,6]. Agricultural and forestry residue, or biomass residue wastes, such as the hard shells of apricot stones, almond, walnut and hazelnut shells, rice hulls etc., can be used as raw materials for activated carbon production [7]. Conversion of these raw materials to activated carbon is one way to add economic value to the raw materials and reduce the large quantity of solid wastes.

Water olive (*Elaeocarpus hygrophilus* Kurz) is a tropical plant, an evergreen shrub that can grow from 3-13 meters tall [8]. In the North-Eastern part of Thailand, water olive trees are found predominately in waterfront

areas and their fruit is available from June to November. The water olive is usually preserved, pickled, and made into compote. The seeds are left as natural solid waste in large quantities and yet are of great value. Because the shell of the water olive seed is hard and woody, it can be considered as an alternative for making activated carbon. Additionally, there is an alternative way to enhance the adsorption capacity of activated carbon by means of adding negatively charged functional groups such as carboxyl groups to the activated carbon surface. This results in higher affinity to the positively charged molecules or ions, which is accomplished by modifying the activated carbon with nitrilotriacetic acid [9].

The acid is also known as "aminopolycarboxylic acid" (APCA) which forms coordination compounds with metal ions (chelates). It is expected that the immobilization of the nitrilotriacetic acid on the activated carbon causes additional carboxyl groups to appear on the adsorbent surface as additional adsorptive sites. In addition, nitrilotriacetic acid is biodegradable in nature and does not pose any disposal issues. Adsorbent modification by nitrilotriacetic acid is primarily used for heavy metal adsorption such as copper (II) ions, chromium (III) and chromium (IV) ions [9,10]. Very few studies have indicated cationic dye adsorption. For example, banana pith modified with nitrilotriacetic acid increased methylene blue uptake from 100 to 142.86 mg/g [11]. The percentage of methylene blue adsorbed on the nitrilotriacetic acid-modified cellulose film was 89.19%, compared to 63.80% on the raw adsorbent [12]. The use of modified activated carbon (MAC) by nitrilotriacetic acid for TT cationic dye adsorption has not been well-documented and is highlighted as a novelty in this work.

This study aims to prepare activated carbon (AC) from local water olive seeds and then modify it by using nitrilotriacetic acid to fix additional negative functional groups such as carboxyl groups [9,10]. An increase in the number of carboxyl groups can strengthen electrostatic attraction. The characteristics of the MAC were investigated to reveal the transformation to carbon adsorbent. Batch adsorption experiments were also carried out with regard to the effects of the initial pH solution, contact time, initial dye concentration, and temperature. The experimental condition with the highest adsorption capacity was evaluated and correlated with well-established kinetic adsorption and adsorption isotherm models.

2. Materials and methods

2.1 Dye and chemicals

TT ($C_{17}H_{19}ClN_2S$) with a molecular weight of 318.86 g/mol was purchased from SIGMA-Aldrich (product no. T3516). It is also known as "basic yellow 1". Its structure is shown in Figure 1 which is a modified version according to the supplier's product information sheet. Nitrilotriacetic acid, $N(CH_2COOH)_3$, was also purchased from SIGMA-Aldrich (CAS no. N8977) with a molecular weight of 191.14. All chemicals were used as received without any further purification.

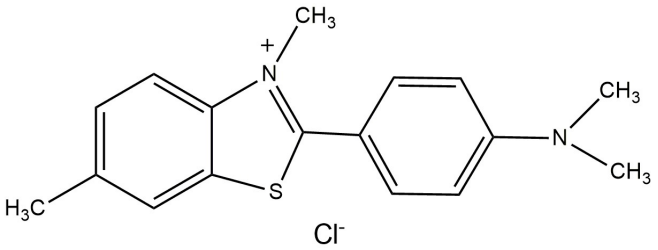

Figure 1 Chemical structure of the TT dye.

2.2 Preparation of AC

Water olive seeds were collected from a local market in Ubon Ratchathani Province, Thailand. The fixed carbon content of the water olive seed was analyzed by the ASTM D3174-12 procedure [11]. It was found that water olive seed had a fixed carbon rate of 48.22%, and it was found that the high carbon content materials could provide a higher yield of AC.

The seed was first washed thoroughly three times with distilled water, then oven-dried at a temperature of 105°C until the weight was constant and was subsequently ground for oil extraction by being soaked in a 95% n-hexane (Merck, Germany) solvent overnight. The oil-free material was dried again in the oven at 105°C. Then, the dried material was carbonized at 450°C for 1 h. The remaining solid, called "char," was naturally cooled by being left in the furnace. The char was further activated by mixing char and KOH (Merck, Germany) as a given mass ratio of 1:3 and then carbonized again at 780°C for 1 h. Carbonization was accomplished with a nitrogen atmosphere. The natural, cooled solid is AC. It was washed three times with 20%v/v HCl (Merck, Germany) to remove the remaining KOH and rinsed with distilled water to ensure that the pH of the rinse water was equal to

the distilled water. The carbon was ground and filtered through a 100-mesh sieve. The AC was stored in a desiccator for further modification.

2.3 Modification of AC

The AC was further modified by immobilization of the nitrilotriacetic acid as a post-treatment step. 15.37 g of the AC was added to 100 mL of 7.7% w/v nitrilotriacetic acid solution contained in an Erlenmeyer flask. The modification of the AC by nitrilotriacetic acid was based on the study of Iannicelli-Zubiani et al. [12]. Then, the mixture was shaken in an incubator shaker (Remi RBS-12, India) at 200 rpm for 24 h. Next, the suspension was vacuum filtered using a microfilter (Whatman 1823-047, Japan) to harvest the modified solid. The solid was then washed repeatedly until the pH of the rinse-distilled water was identical to that of the distilled water. The solid was dried in an oven at 105°C for 24 h (or until the weight was constant). The final solid MAC was stored in the desiccator for future use.

The MAC was characterized using an automatic surface analyzer (ASI-C-8, Quantachrome Instrument) at 77K to determine N_2 adsorption-desorption. The specific surface area, average pore size, and total pore volume were determined using the Brunauer-Emmett-Teller (BET)-method, Barrett-Joyner-Halenda (BJH) method, and the amount of N_2 adsorbed at 0.95 relative pressure. A Field Emission Scanning Electron Microscope (FESEM, JSM-541OLV, LEO) at 20 kV with 500x-5,000x magnification was used to measure the chemical composition of the MAC and adsorbent morphology. The functional groups of the adsorbent were determined using a Fourier Transform Infrared Spectrophotometer (FTIR) (Spectrum RX1, Perkin Elmer) with a wave number ranging from 4,000 to 400 1/cm. The point of zero charge (pHpzc) was also discovered. An amount of 0.1 g adsorbent was added into 0.1 M NaCl solution, and the initial pH solution was adjusted to 2, 4, 6, 8, and 10 using 0.1 M HCl and/or 0.1 M NaOH. The suspension was mixed at 200 rpm for 24 h under 30°C. In the final step, the pH solution was measured and the pHpzc was located at the abscissa-intercept of the plot between pH_0-pH_f versus pH_0.

2.4 Batch adsorption experiments

The batch adsorption tests were carried out as functions of initial pH, contact time, initial dye concentration, and temperature. Firstly, the influence of initial pH was investigated. A group of Erlenmeyer flasks was filled with 100 mL of the 150 mg/L dye solution. The pH of the solutions was adjusted between 2.0-10.0 by adding 0.1M NaOH (Qrec, New Zealand) and/or 0.1M HCl. The adsorbent (0.1g) was added into the dye solutions and then the mixtures were shaken at a controlled temperature of 30°C for 24 h. The removal of the adsorbent from the suspension was performed by using vacuum filtration, and the filtrate was subjected to the UV Vis Spectrophotometer for measuring the absorbance at a maximum wavelength (λ_{max}) of 446 nm. The absorbance was converted to the concentration by the calibration curve (the plot of absorbance vs. dye concentration).

Secondly, the effect of contact time was studied. Another set of Erlenmeyer flasks containing 100 mL of 150 mg/L dye solutions was prepared. The pH of the solutions was adjusted to 4.0. The adsorbent (0.1 g) was put into the dye solutions and then the mixtures were shaken at a controlled temperature of 30°C. The samples were measured at time intervals of 10-600 min. The final dye concentration was evaluated in the same manner as that of the first experiment.

Thirdly, a set of Erlenmeyer flasks containing 100 mL of 50-300 mg/L dye solutions was prepared to study the effect of the initial dye concentration. The pH of the solutions was adjusted to 4.0. The procedure was carried out according to the same methods as those in the first experiment.

Finally, the influence of temperature on the adsorption was performed. The final test was carried out in the same manner as that in the first experiment, but the pH was fixed at 4.0 and the temperature varied between 30-60°C. In addition, another experiment on the adsorption at a temperature of 60°C was investigated to compare the dye uptake of the MAC and the unmodified AC.

3. Results and discussion

3.1 Characteristics of MAC

The N_2 adsorption-desorption isotherm at 77 K of the MAC is shown in Figure 2. A Type I isotherm classified by IUPAC was identified from the isotherm curve. Normally, a Type I isotherm is found in microporous materials [13] and that the AC is a microporous material is well-documented [14]. The BET method determined the specific surface areas of the MAC and AC were 605.60 m^2/g and 29.97 m^2/g, respectively. Table 1 summarizes the specific surface areas of the activated carbon derived from various sources. The properties of MAC and the activated carbon were comparable. The average pore size of the MAC was 1.17 nm, which is considered a microporous material because the pore size is less than 2.0 nm. In addition, the total pore volume evaluated from t-plots was 0.3274 cm^3/g.

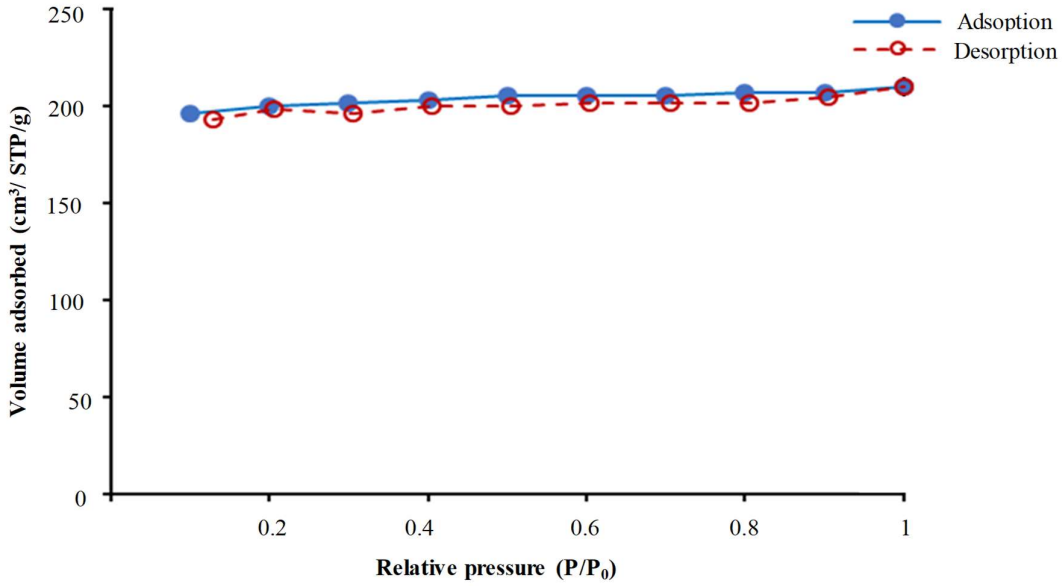

Figure 2 N_2 adsorption-desorption isotherm of the MAC at 77 K.

Table 1 Specific surface area of activated carbon from various sources.

Adsorbent	Specific surface area (m^2/g)	Reference
Activated carbon from sewage sludge	372	[15]
Activated carbon from rubber fruit shell	456	[16]
Activated carbon from plant waste	738	[17]
Activated carbon from walnut shell waste	882	[18]
Activated carbon from coconut shell	437	[19]
Activated carbon from pine sawdust	962	[20]
MAC	605.60	This study
AC	29.92	This study

The IR spectra of the AC are illustrated in Figure 3. Vibration bands were observed at 3,467.44 1/cm O-H stretching (alcohols or phenols), 2,935 1/cm O-H stretching (carboxylic acids), 2,894.68 1/cm C-H stretching (alkane), 2,372.10 1/cm C=C stretching (alkyne) or C≡N stretching (nitrile), 1,668 1/cm C=O stretching (carbonyl), 1,594 1/cm N-H bending (1° amine) or C-C stretching (aromatics) and 1,072.25 1/cm C-O stretching (carboxylic acids) [21]. Carboxyl groups attached to the external surface of the MAC were expected and were attributed to the immobilization of the nitrilotriacetic acid on the AC surface.

The interactions between the TT and MAC are classified into 2 categories: van der Waals forces and electrostatic forces. The van der Waals forces are the interactions among the carbon and other adsorbate molecules, which can occur with any kind of molecule. The electrostatic attraction can be represented by the interactions between carboxyl groups on the MAC and the positively charged TT molecules.

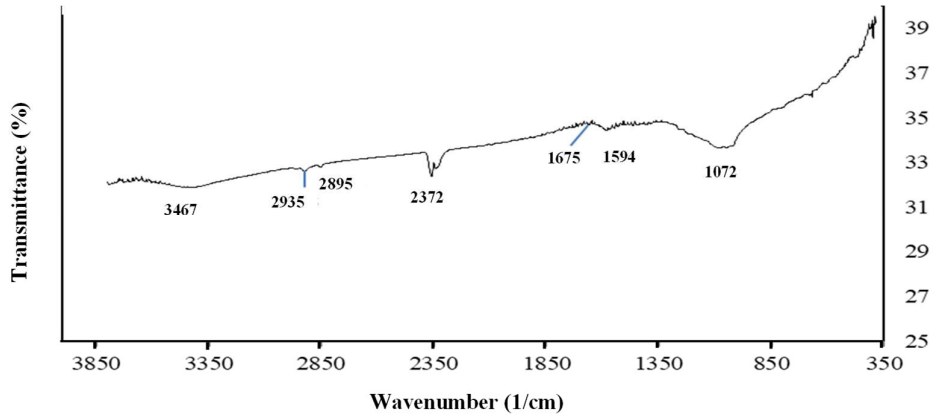

Figure 3 FT-IR analysis of the MAC.

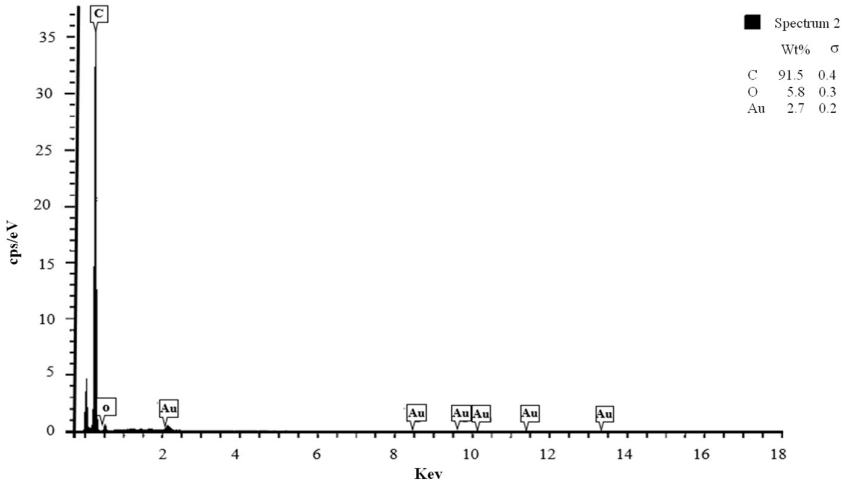

Figure 4 EDS result of the MAC.

EDS (Energy-dispersive X-ray) analysis of the MAC is depicted in Figure 4. It revealed that the major component of the adsorbent was carbon, in accordance with the high fixed carbon content of the water olive seed noted above. The nitrogen element in the nitrilotriacetic acid molecule was small (1 atom/molecule) so there was no nitrogen content in the EDS result and this result was similar to a prior study [22].

The scanning electron microscope (SEM) images with different enlargement degrees of the MAC are illustrated in Figure 5. A tremendous number of pores were observed distributed uniformly over the MAC particle (Figure 5 A). Figure 5 (B), 5 (D) exhibited more enlarged SEM images revealing the distribution of various macropores (pore sizes exceeding 50 nm) along the external surface of the MAC. Additionally, the interior of those macropores contained a number of smaller pores. The result was in line with similar carbonaceous materials [23,24].

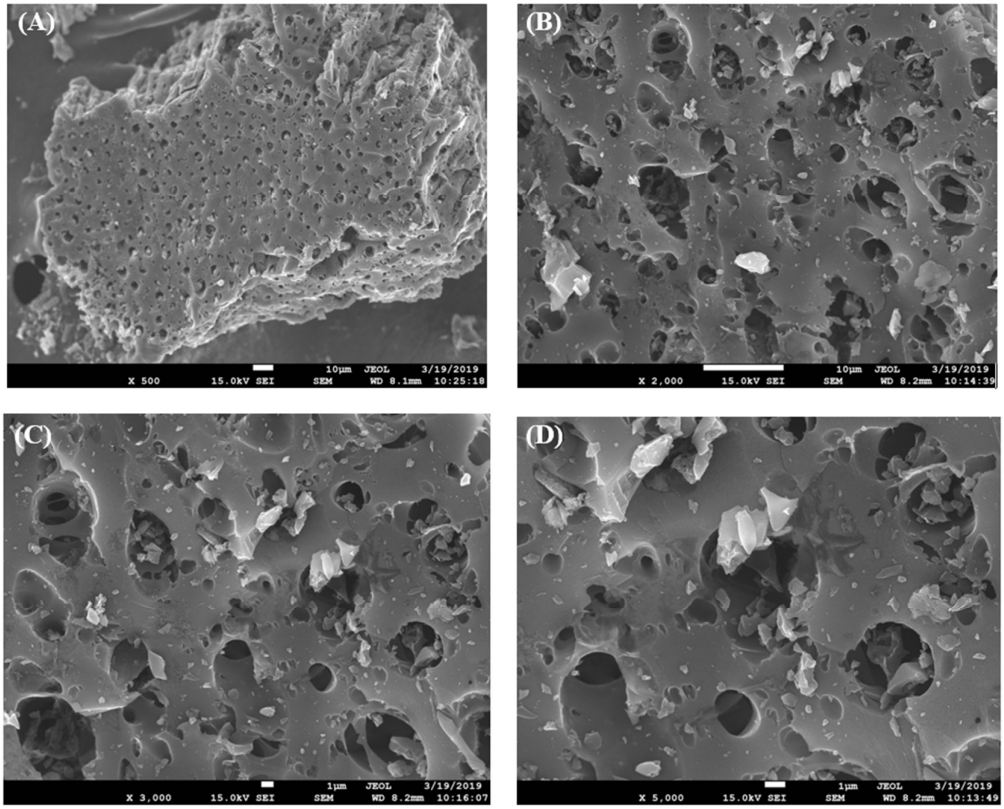

Figure 5 SEM images of the MAC at varying degrees of enlargement; (A) 500x, (B) 1000x, (C) 3000x, and (D) 5000x.

3.2 Influence of factors affecting the adsorption

The adsorption capacity of the MAC increased with a corresponding increase of the initial pH solution (Figure 6). A similar result was also discovered in related prior research [25,26]. From the adsorbent characteristics, the results revealed that there were negative functional groups existing on the adsorbent surface. The TT molecule contained three structural fragments: (1) a benzyl ring, (2) a benzothiazole ring, and (3) the dimethylamino group as illustrated in Figure 1. In general, the TT molecule had a positive charge (+1e) on the N atom (N8) that was not uniformly distributed among the molecule fragments [27]. At the low pH, these negative functional groups did not completely dissociate so it mostly stayed in a neutral form. Physical adsorption is dominant due to the high specific surface area of the MAC. In addition, the competition between the H^+ and the TT cationic dye may cause low dye uptake. At the higher pH, the functional groups became more dissociated and remain in a negatively charged form. The more dissociated functional group contributes to the higher electrostatic interaction between the positive charge of TT dyes and the negative charge of the MAC. Thus, the electrostatic interaction becomes dominant. Also, the higher adsorption capacity results from the fact that there is less competition between the dye and H^+. In an alkaline medium, the fraction of H^+ is low while the OH^- is high.

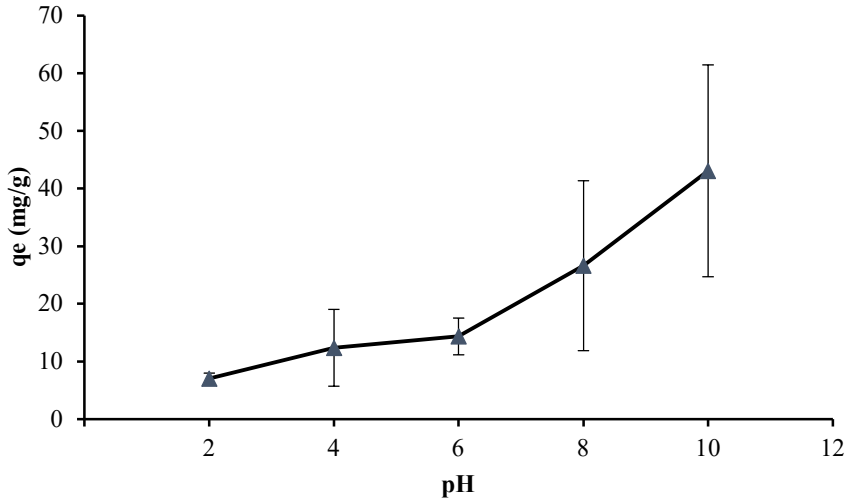

Figure 6 Adsorption capacity of TT dyes on the MAC at different initial pH solutions.

An increase in contact time caused an increase in the dye uptake on the MAC. The adsorption rate was fast in the first 15 min and slowed during the second stage (15-240 min) and then finally leveled off at 240 min as shown in Figure 7. The rapid increase in the first stage comes from the fact that there are numerous adsorptive sites available on the external surface of the adsorbent for the TT removal [28], for the dye molecules can occupy those surfaces easily. The adsorptive sites loaded by the TT molecules are mostly saturated. Subsequently, the dye molecules diffuse into the interior of the adsorbent leading to a slower rate of dye uptake as it is affected by the internal mass transfer resistance [29]. Consequently, all adsorptive sites become saturated at 240 min which is then set as the equilibration time.

A reduction in dye adsorbed on the MAC was caused by an increase in the initial dye concentration (Figure 8). Two hypotheses describe this result. Firstly, adsorption inside the pores of the AC is mostly dominated by a diffusion process. The driving force in such a case is the chemical potential gradient of the dye species. The chemical potential of a species is defined as “absorbed” or “released energy” due to changes in the number of particles from the given species. Under special conditions, the interactions among molecules of the dye are attractive leading to a reduction in the chemical potential at a certain dye concentration. In such a case, increasing the initial dye concentration would result in a further reduction of the chemical potential. Another possible explanation is a surface saturation effect. After acceleration during a short period of time, the transfer is decreased by congestion at the entrance pores. Therefore, the fraction of dyes removed decreases when the initial dye concentration increases, which is in accord with prior literature [30,31].

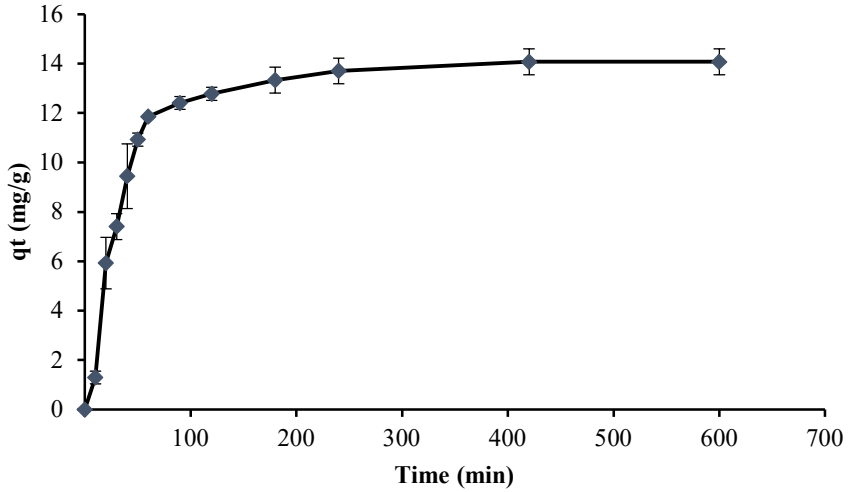

Figure 7 Dye removal of the TT on the MAC at different contact times.

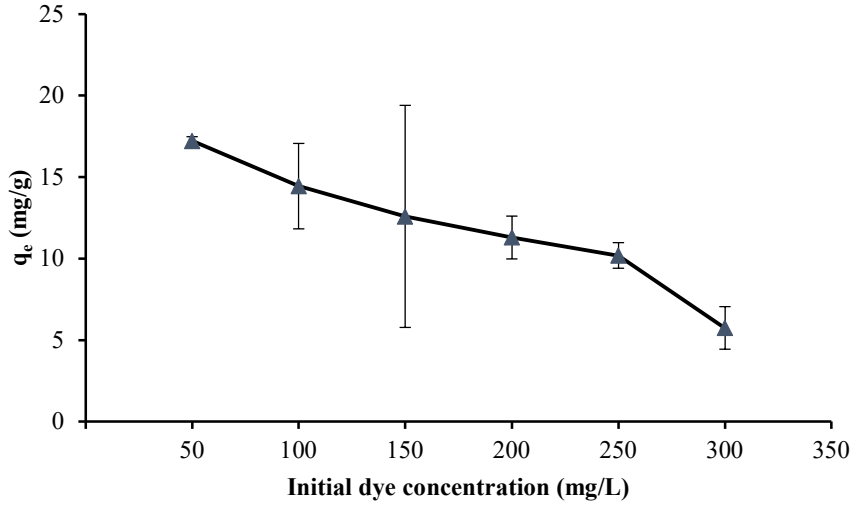

Figure 8 Dye removal of the TT on the MAC at different initial dye concentrations.

The number of dye particles adsorbed on the MAC increased with an increase in the temperature as shown in Figure 9. This indicated that the larger number of dye particles became embedded in the adsorbent when the temperature was raised. We can say that the adsorption involves chemical reactions and is an endothermic process. More energy input causes a higher equilibrium constant, and the reaction is forward [32]. Additionally, an increase in the temperature causes physical changes in the adsorbent and the dye molecules can diffuse into the pores more easily and occupy more active sites inside the pores of the adsorbent. From the above results, the highest adsorption capacity of the TT dye on the MAC was 43.09 mg/g observed under a certain condition: pH_0 of 10.0, with a contact time of 240 min, a dye concentration of 50 mg/L and a temperature of 60°C.

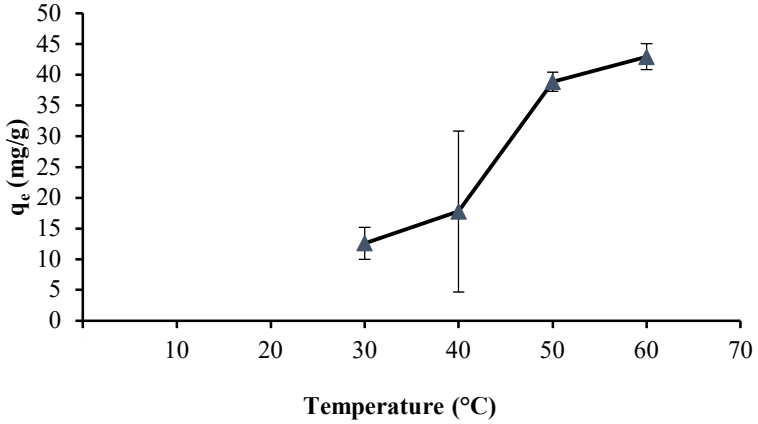

Figure 9 Dye removal of the TT on the AC at different temperatures.

An additional experiment involved adsorption of the TT dye on the AC under certain conditions that were tested: a pH_0 of 4.0, a contact time of 240 min, an initial dye concentration of 150 mg/L and a temperature of 60°C. The result was compared to that of the MAC. It was found that the TT dye uptakes on the AC and MAC were 56.68 and 42.96 mg/g, respectively. Surprisingly, the modification of the AC in this study caused a reduction in dye removal efficiency. The addition of organic acid to the AC may increase the overall charge distribution over the adsorbent surface as well a number of the new adsorption sites. This is advantageous for metal adsorption but not for dye adsorption because dye molecules are larger and better adsorbed on a surface with a low charge distribution [33,34]. In this study, the modification of the AC by nitrilotriacetic acid caused an increase in pHpzc from 5.3 to 7.6, resulting in a higher surface charge density.

3.3 Kinetic adsorption modeling

Adsorption mechanisms of the dye molecules involve several stages. In the first stage, the dye molecule is transported from the solution to the stagnant film covering the adsorbent. Then, it diffuses through the stagnant film and binds to the external surface of the adsorbent. The dye molecule is later transported to the pore and is adsorbed into the interior surface of the adsorbent. The rate of the limiting step is usually the stage taking the longest to identify. There are several kinetic models which are used as tools to determine the rate of the limiting step, such as pseudo-first order and pseudo-second order kinetic models, and intraparticle kinetic models.

The pseudo-first order kinetic model was proposed by Lagergren [35]. This model was developed based on a homogeneous reaction to fit the kinetic data of the heterogeneous reaction and the 'pseudo' is addressed as a prefix. The linear form of this model can be expressed as:

$$\ln(q_e - q_t) = \ln(q_e) - k_1 t \quad (1)$$

where q_e and q_t (mg/g) are the adsorption capacity at the equilibrium stage and at instantaneous time *t*, respectively. The k_1 is first order rate constant (1/min) and t is time (in minutes). If the chemical reaction is the rate-controlling step, the measurement data will follow the pseudo-first order reaction model. This model usually accords well with the first 30 min of the experimental data.

The pseudo-second order kinetic model was proposed by Ho and McKay [36]. This model was developed based on the second order homogeneous reaction to fit the kinetic data of the heterogeneous reaction and the 'pseudo' is addressed as a prefix. The linear form of this model can be expressed as:

$$t/q_t = 1/(k_2.q_e^2) + t/q_e \quad (2)$$

where k_2 is second order rate constant (g/(mg*min)). If the chemical reaction is the rate-controlling step, the measurement data follows the pseudo-second order reaction model.

The intra-particle diffusion model was developed by Weber and Morris [37] and is used to describe the transport property of metal ions from the solution to the interface, which can be expressed as:

$$q_t = k_p.t^{0.5} + C \quad (3)$$

where k_p is the intraparticle rate constant (mg/(g*min$^{0.5}$)) and C is the constant value or an intercept of the straight line (mg/g) providing information on the boundary layer thickness. The kinetic data fit best with the pseudo-second order reaction model (R^2>0.98) indicating that the formation of interactions between dye molecules and the MAC surface is the rate of the limiting step. The model constants of the three well-established models are presented in Table 2.

Table 2 Kinetic parameters for adsorption of the TT on the MAC.

Kinetic adsorption model	Parameter	Value
Pseudo-first order reaction	$q_{e\ (exp)}$, mg/g	14.07
	k_1, 1/min	0.01
	$q_{e,\ (Cal)}$, mg/g	9.35
Pseudo-second order reaction	R^2	0.91
	k_2, g/(mg*min)	0.00
	$q_{e,\ (Cal)}$, mg/g	14.99
	R^2	0.98
Intraparticle diffusion*	k_p, mg/(g*min$^{0.5}$)	0.02
	C, mg/g	11.44
	R^2	0.96

*Only the experimental data in the last stage was exhibited (t>30 min).

3.4 Adsorption isotherm

Adsorption behavior is essential because it is used to classify the patterns of dye molecules binding on the adsorbent surface whether they are either monolayer or multilayer in coverage. The adsorption isotherm is the relationship between equilibrium quantities of the dyes adsorbed on the adsorbent (mg/g) and the equilibrium dye concentration (mg/L). There are several isotherm models used to describe the adsorption behavior, e.g., the Langmuir and Freundlich isotherm equations.

The Langmuir isotherm [38] was developed based on the assumption that the adsorbent surface is homogeneous or has a finite number of identical sites. The Langmuir isotherm equation in linear form is written as:

$$C_e/q_t = C_e/q_m + 1/k_L.q_m \quad (4)$$

where k_L is the Langmuir constant (L/g), C_e is the concentration at the equilibrium stage and q_m is the maximum monolayer adsorption capacity (mg/g). The important characteristics of the Langmuir isotherm are explained by "R_L" as a "dimensionless constant". The R_L is an equilibrium parameter or separation factor which can be defined as:

$$R_L = 1/(1+K_L.C_0) \quad (5)$$

This parameter suggests that this type of isotherm is irreversible (R_L = 0), favorable (0<R_L<1), linear (R_L=1), or unfavorable (R_L>1). The Freundlich isotherm [39] was developed under the assumption that the adsorbent surface is heterogeneous or has diverse sites. The Freundlich isotherm equation in linear form is written as:

$$\ln(q_e) = \ln(k_F) + (1/n)\ln(C_e) \quad (6)$$

where k_F and n are physical constants of the Freundlich isotherm (mg$^{1-1/n}$.L$^{1/n}$/g). The k_F and n indicates adsorption capacity and adsorption intensity, respectively.

The Temkin isotherm is a model focused on adsorbent-adsorbate interactions. It is based on the assumption that the heat of adsorption (a function of temperature) of all molecules in the layer decreases linearly rather than logarithmically according to the surface coverage. As implied in the equation, its derivation is characterized by a uniform distribution of binding energies (up to a certain maximum binding energy) and performed by plotting the adsorption capacity (q_e) against the natural logarithm of the concentration at the equilibrium stage ($\ln(C_e)$). The model is demonstrated by the following equations [40]:

$$q_e = (RT/b_T)\ln(A_TC_e) \quad (7)$$

$$q_e = B\ln(A_T) + B\ln(C_e) \quad (8)$$

A_T is the Temkin isotherm equilibrium binding constant (L/g) and b_T is the Temkin isotherm constant (J/mol). R is the gas constant (8.341 J/mol·K) and T is the absolute temperature at 303 K. B is the constant related to the heat of sorption and defined by the expression $B = RT/b_T$.

The Langmuir and Temkin isotherms closely matched the experimental data as presented in Table 3. The Langmuir isotherm model reveals that the monolayer coverage of the TT dye molecules takes place on the surface of the adsorbent. The adsorption capacity (q_m) of the TT dye molecules on various adsorbents is presented in Table 4. Furthermore, the Temkin isotherm indicates a physical adsorption process.

Table 3 Isotherm parameters for the adsorption of the TT on the MAC.

Adsorption isotherm model	Parameter, unit	Value
Langmuir isotherm	k_L, L/g	0.16
	q_m, mg/g	6.18
	R_L (-)	0.04
	R^2	0.84
Freundlich isotherm	k_F, $(mg^{1-1/n*}L^{1/n})/g$	69.25
	n	-2.65
	R^2	0.72
Temkin isotherm	b_T, J/mol	-595.54
	B	-4.23
	R^2	0.85
	A_T, L/g	$4.86x10^{-4}$

3.5 Adsorption mechanisms

The possible interactions between the adsorbent and the dye molecules are shown in Figure 10. The symbol 1 shows the adsorption of TT dye molecules on the external surface of the MAC. The adhesion of the hydrophobic TT dye molecules and the hydrophobic aspect of the MAC involve van der Waals forces which normally take places for all types of molecules [41]. The symbol 2 represents the diffusion of TT dye molecules at the internal surface or the pore of the MAC. This step is usually slow due to the internal mass transfer resistance. A slow increase in the dye uptake with a long contact time in the second stage was mentioned earlier in Figure 7. Symbol 3 represents electrostatic attraction between the additional carboxyl groups of the nitrilotriacetic acid and the positive functional groups of the TT dye molecules. Further discussion about electrostatic interactions between the fixed negative charge on the adsorbent surface and the cations can be found elsewhere [42]. In addition, another experimental result in this study in accordance with the electrostatic interactions revealed an increase in the dye uptake caused by an increase in the solution pH. At a higher pH, the carboxyl groups become more dissociated, and electrostatic interactions are strengthened.

Table 4 Adsorption capacity of the TT on various adsorbents.

Adsorbent	Adsorption capacity (mg/g)	References
Rhytidiadelphus squarrosus	126	[43]
Magnetic *Rhytidiadelphus squarrosus*	154	[44]
Vesicularia dubyana moss	119	[45]
Modified montmorillonite	95	[46]
AC	56.68	This study
MAC	43.09	This study

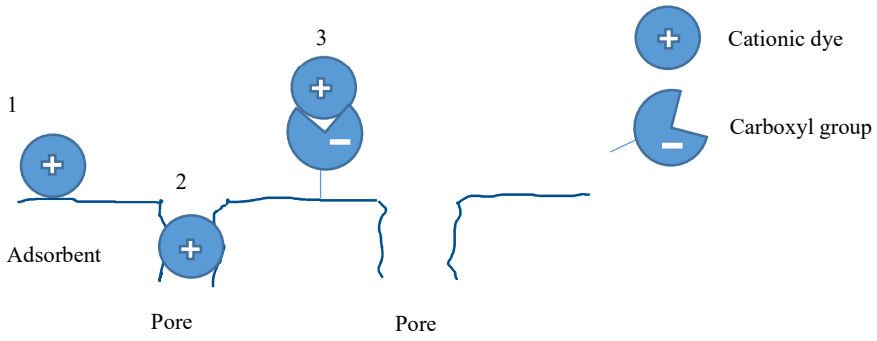

Figure 10 Schematic representation of TT dye molecules adsorbed on the MAC.

4. Conclusion

The MAC prepared from water olive seeds (*Elaeocarpus hygrophilus* Kurz) is a microporous material which has a higher specific surface area compared to the AC. The MAC contains fixed negative charges on the external surface which is strongly attractive to the cationic molecules. The removal efficiencies of TT dyes, cationic dyes, increased with an increase in pH_0, contact time, and temperature but decreased with an increase in the initial dye concentration. The optimum condition for TT removal was suggested at a certain condition: an initial pH of 10.0, a contact time of 240 min, an initial dye concentration of 50 mg/L, and a temperature of 60°C. The immobilization of the nitrilotriacetic acid reduced TT dye uptake due to an increase in pHpzc, but significantly increased the specific surface area of the MAC, which possibly increased sorption toward other pollutants.

5. Acknowledgements

The authors would like to thank the Faculty of Engineering, Ubon Ratchathani University, for partial financial support and express our gratitude to the National Research Council of Thailand in 2020 for further financial support.

6. References

[1] Auemporn J, Kanokkorn S, Angkhana I, Ratchaneeporn N, Benjamas O, Wattana T, et al. Diversity and traditional knowledge of textile dyeing plants in northeastern Thailand. Econ Bot. 2017;71:241-255.

[2] Xue C, Lin YT, Chang D, Guo Z. Thioflavin T as an amyloid dye: fibril quantification, optimal concentration and effect on aggregation. R Soc Open Sci. 2017;4(1):160696.

[3] Pai S, Srinivas KM, Selvaraj R. A review on adsorptive removal of dyes from wastewater by hydroxyapatite nanocomposite. Environ Sci Pullut Res. 2021;28:11835-11849.

[4] Malmos KG, Mejia BLM, Weber B, Buchner J, Alvarado RM, Naiki H, et al. ThT 101: a primer on the use of Thioflavin T to investigate amyloid formation. Amyloid. 2017;24:1-16.

[5] Leon M, Silva J, Carrasco S, Barrientos N. Design, cost estimation and sensitivity analysis for a production process of activated carbon from waste nutshells by physical activation. Processes. 2020;8(8): 945.

[6] Nandiyanto A. Cost analysis and economic evaluation for the fabrication of activated carbon and silica particles from rice straw waste. JESTEC. 2018;13:1523-1539.

[7] Mohammad AAG, Sweleh AO. Optimizing textile dye removal by activated carbon prepared from olive stones. Environ Technol Innov. 2019;16:100488.

[8] Damtab J, Nutaratat P, Boontham W, Srisuk N, Duangmal K, Yurimoto H, et al. *Roseomonas elaeocarpi* sp. Nov., isolated from olive (*Elaeocarpus hygrophilus* Kurz.) phyllosphere. Int J Syst Evol Microbiol. 2016;66(1):474-480.

[9] Saini S, Arora S, Kirandeep B, Singh BP, Katnoria JK, Kaur I. Nitrilotriacetic acid modified bamboo charcoal (NTA-MBC): an effective adsorbent for the removal of Cr (III) and Cr (VI) from aqueous solution. J Environ Chem Eng. 2018;6(2):2964-2974.

[10] Saini S, Katnoria JK, Kaur I. Surface modification of *Dendrocalamus strictus* charcoal powder using nitrilotriacetic acid as a chelating agent and its application for removal of copper (II) from aqueous solutions. Sep Sci Technol. 2021;56:275-289.

[11] Nayeri D, Mousavi SA. Dye removal from water and wastewater by nanosized metal oxides-modified activated carbon: a review on recent researches. J Environ Health Sci Engineer. 2020;18:1671-1689.

[12] Zubiani IEM, Stampino PG, Cristiani C, Dotelli G. Enhanced lanthanum adsorption by amine modified activated carbon. Chem Eng J. 2018;341:75-82.

[13] Gecgel U, Uner O, Gokara G, Bayrak Y. Adsorption of cationic dyes on activated carbon obtained from waste *Elaeganus* stone. Adsorp Sci Technol. 2016;34(9-10):512-525.

[14] Lin Y, Ma J, Liu W, Li Z, He K. Efficient removal of dyes from dyeing wastewater by powder activated carbon charcoal/titanate nanotube nanocomposites: adsorption and photoregeneration. Envrion Sci Pollut Res. 2019;26:10263-10273.

[15] Almahbashi NMY, Kutty SRM, Ayoub M, Noor A, Salihi IU, Nini AA, et al. Optimization of preparation conditions of sewage sludge based activated carbon. Ain Shams Eng J. 2021;12(2):1175-1182.

[16] Suhdi S, Wang SC. The production of carbon nanofiber on rubber fruit shell-derived activated carbon by chemical activation hydrothermal process with low temperature. Nanomaterials. 2021;11:2038.

[17] Kishibayev KK, Serafin J, Tokpayev RR, Khavaza TN, Atchabarova AA, Abduakhytova DA, et al. Physical and chemical properties of activated carbon synthesized from plant wastes and shungite for CO_2 capture. J Environ Chem Eng. 2021;9(6):106798.

[18] Khoshraftar Z, Ghaemi A. Presence of activated carbon particles from waste walnut shell as a biosorbent in monoethanolamine (MEA) solution to enhance carbon dioxide absorption. Heliyon. 2021:e08689.
[19] Daouda AMM, Akowanou OAV, Mahunon RSE, Adjinda CK, Aina MP, Drogui P. Optimal removal of diclofenac and amoxicillin by activated carbon prepared from coconut shell through response surface methodology. South African J Chem Eng. 2021;38:78-89.
[20] Yang Y, Cannon FS. Biomass activated carbon derived from pine sawdust with steam bursting pretreatment; perfluorooctanoic acid and methylene blue adsorption. Bioresour Technol. 2022;344(A): 126161.
[21] Yadav S, Asthana A, Chakraborty R, Jain B, Singh AK, Carabineiro SAC, et al. Cationic dye removal using novel magnetic/activated charcoal/β-cyclodextrin/alginate polymer nanocomposite. Nanomaterials. 2020;10:170.
[22] Adewuyi A, Pereira FV. Nitrilotriacetic acid functionalized *Adansonia digitata* biosorbent: preparation, characterization and sorption of Pb (II) and Cu (II) pollutants from aqueous solution. J Adv Res. 2016;7(6):947-959.
[23] Moosavi S, Lai CW, Gan S, Zamiri G, Pivehzhani OA, Johan MR. Application of efficient magnetic particles and activated carbon for dye removal from wastewater. ACS Omega. 2020;5(33):20684-20697.
[24] Nizam NUM, Hanafiah MM, Mahmoudi E, Halilm AA, Mohammad AW. The removal of anionic and cationic dyes from an aqueous solution using biomass-based activated carbon. Sci Rep. 2021;11:8623.
[25] Zhou Y, Wang Z, Hursthouse A, Ren B. Gemini surfactant-modified activated carbon for remediation of hexavalent chromium from water. Water. 2018;10:91.
[26] Shu J, Cheng S, Xia H, Zhang L, Peng J, Li C, et al. Copper loaded on activated carbon as an efficient adsorbent for removal of methylene blue. RSC Adv. 2017;7:14395-14405.
[27] Sulatskaya AI, Maskevich AA, Kuznetsova IM, Uversky VN, Turoverov KK. Fluorescence quantum yield of Thioflavin T in rigid isotropic solution and incorporated into the amyloid fibrils. PLoS ONE. 2010;5:e15385.
[28] Phothitontimongkol T, Kumaiard N, Tantipalakul Y. Activated carbon from tamarind wood supported TiO_2 for methylene blue dye removal in wastewater by photocatalytic process. Burapha Sci J. 2016; 21(3):73-91.
[29] Ghani ANT, Chaghaby EGA, Rawash ESA, Lima EC. Adsorption of coomassie brilliant blue R-250 dye onto novel activated carbon prepared from *Nigella Saiva* L. waste: equilibrium, kinetics and thermodynamics running title: adsorption of brilliant blue dye onto *Nigella Sativa* L. waste activated carbon. J Chil Chem Soc. 2017;62(2):3505-3511.
[30] Sivaprakash S, Kumar PS, Krishan SK. Adsorption study of various dyes on activated carbon Fe_3O_4 Magnetic nanocomposite. Int J Appl Chem. 2017;13(2):255-266.
[31] Bello OS, Adegoke KA, Sarumi OO, Lameed OS. Functional locust bean pod (*Parkia biglbosa*) activated carbon for rhodamine B dye removal. Heliyon. 2019;5:e02323.
[32] Firdaus NL, Krisnanto N, Alwi W, Muhammad R, Serunting MA. Adsorption of textile dye by activated carbon made from rice straw and palm oil midrib. Aceh Int J Sci Technol. 2017;6(1):1-7.
[33] Tsamo C, Kidwang GD, Dahaina DC. Removal of rhodamine B from aqueous solution using silica extracted from rice husk. SN Appl Sci. 2020;2:256
[34] Tasmo C, Tchouanyo DJH, Meali DS. Treatment of red mud with distilled water to improve its efficiency to remove methylene blue from aqueous solution. IRJPAC. 2017;15(3):1-19
[35] Lagegren SK. About the theory of so-called adsorption of soluble substances. Sven Vetenskapsakad Handingarl. 1989;24(4):1-39
[36] Ho YS, McKay G. Sorption of dye from aqueous solution by peat. Chem Eng J. 1998;70:115-124.
[37] Weber WJ, Morris JC, Sanit J. Kinetics of adsorption on carbon from solution. J Sanit Eng Div ASCE. 1963;18:31-42.
[38] Langmuir I. The adsorption of gases on plane surfaces of glass, mica and platinum. J Am Chem Soc. 1918;40:1361-1368.
[39] Freundlich HMF. Uber die adsorption in losangen. Z Phys Chem. 1906;57:385-470.
[40] Tempkin MI, Pyzhev V. Kinetics of ammonia synthesis on protonated iron catalyst. Acta Physicochem USSR. 1940;12:217-222.
[41] Cai Y, Liu L, Tian H, Yang Z, Luo X. Adsorption and desorption performance and mechanism of tetracycline hydrochloride by activated carbon-based adsorbents derived from sugar cane bagasse activated with $ZnCl_2$. Molecules. 2019;24:4534.
[42] Budsaereechai S, Kamwialisak K, Ngernyen Y. Adsorption of lead, cadmium and copper on natural and acid activated bentonite clay. KKU Res J. 2012;17(5):800-810.
[43] Remenarova L, Pipiska M, Hornik M, Augustin J. Sorption of cationic dyes from aqueous solutions by moss *Rytidiadelphus squarrosus*: kinetics and equilibrium studies. Nova Biotechnol. 2009;9:53-61.

[44] Pipiska M, Zarodnanska S, Hornik M, Duriska L, Holub M, Safarik I. Magnetically functionalized moss biomass as biosorbent for efficient Co^{2+} ions and thioflavin T removal. Materials. 2020;13(16):3619.
[45] Pipiska M, Valica M, Partelova D, Hornik M, Lesny J, Hostin S. Removal of synthetic dyes by dried biomass of freshwater moss *Vesicularia dubyana*: a batch biosorption study. Environments. 2018;5(1):10.
[46] Shin WS. Competitive sorption of anionic and cationic dyes onto cetylpyridinium-modified montmorillonite. J Environ Sci Health A. 2008;43(12):1459-1470.